Supplementary Information

Governing Factors in Mildly Acidic Zn/MnO_2 Batteries: Interplay of Electrochemical Protocols, Electrolyte Composition, and Cell Configuration

Aldina Sultana, Alan Ferris, Colton King, Seongbak Moon,
and Veronica Augustyn*

Department of Materials Science and Engineering
North Carolina State University
Raleigh, NC 27695 (USA)

* corresponding author e-mail: vaugust@ncsu.edu

Table of Contents

1. Supplementary Figures

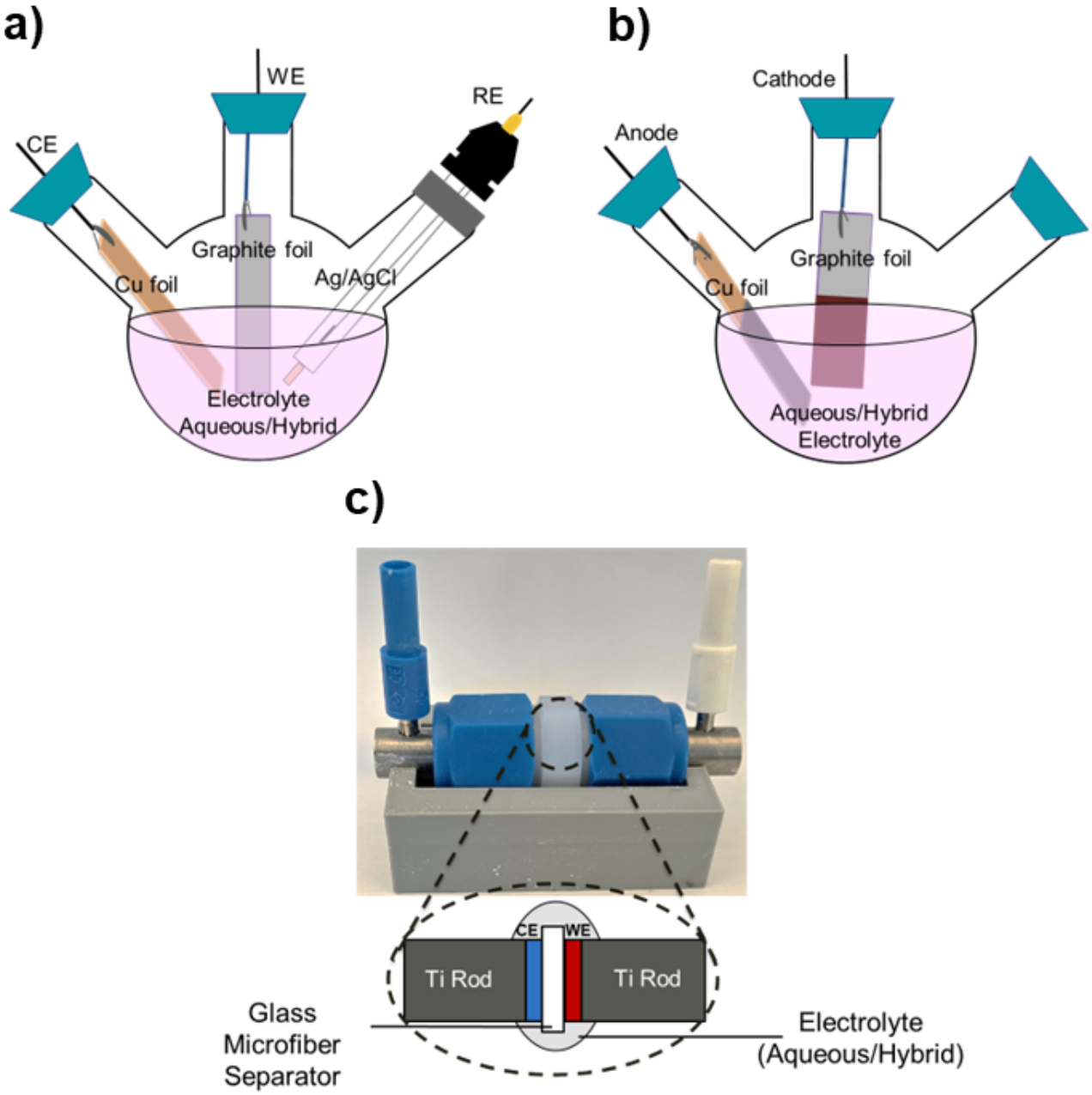

Figure S1. Schematics of electrochemical cells used in this work: a) three electrode flooded electrolyte beaker cell, b) two electrode flooded electrolyte beaker cell, and c) two electrode Swagelok cell.

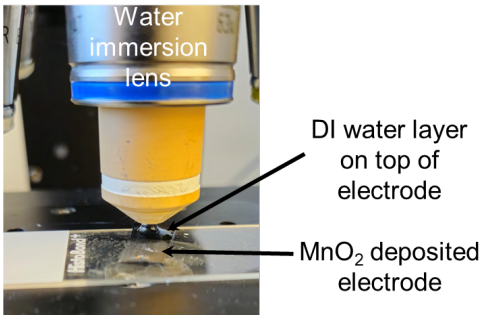

Figure S2. Optical image of the ex-situ Raman spectroscopy sample setup used to mitigate dehydration of the MnO_2 cathode.

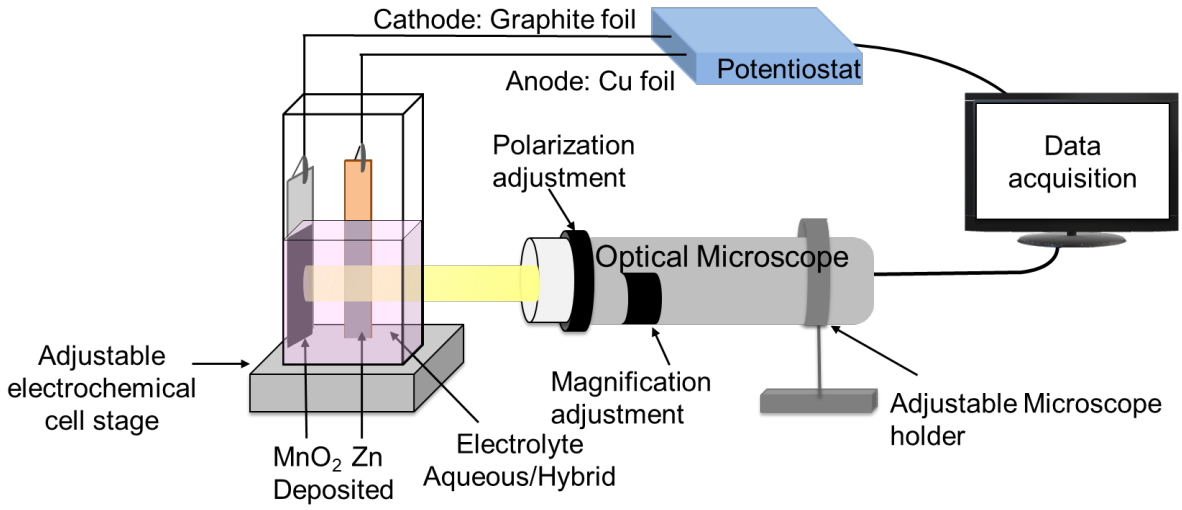

Figure S3. Schematic of the operando electrochemical optical microscopy (EC-OM) setup.

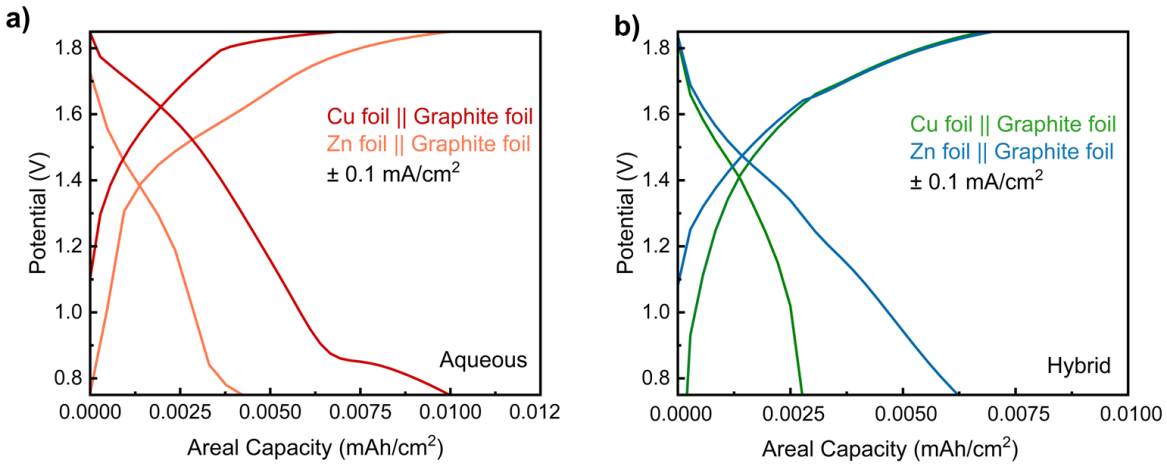

Figure S4. Electrochemical cell configuration and electrolyte affect coulombic efficiency of the Zn/MnO_2 two electrode cell: a) Comparison of a Cu foil vs. Zn foil anode in aqueous electrolyte and b) comparison of the same electrodes in a hybrid electrolyte. In both cases, the cathode current collector was graphite foil and the applied current was +/- 0.1 mA/cm^2.

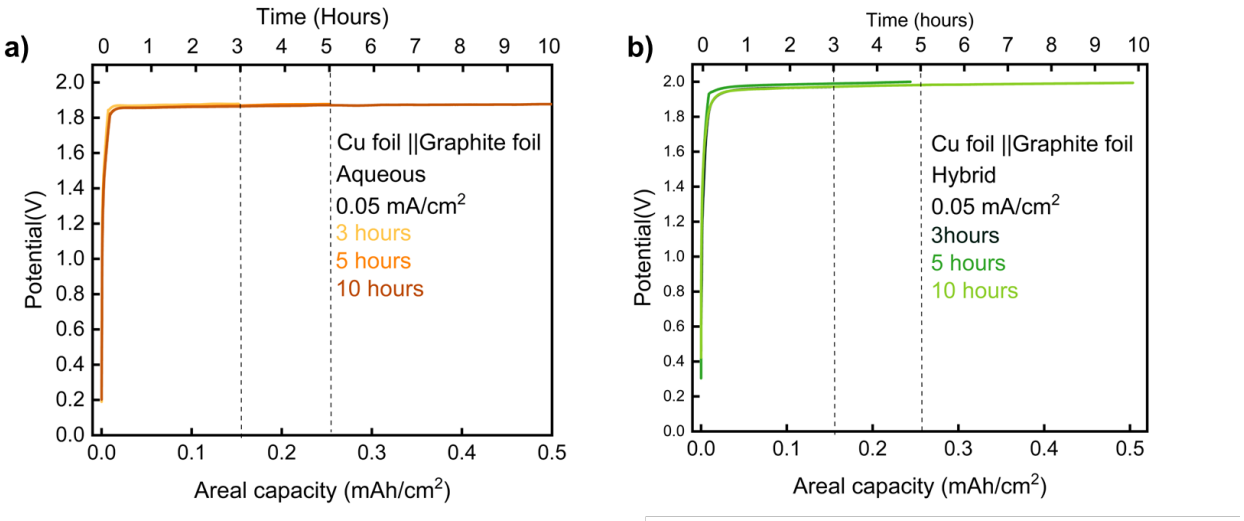

Figure S5. Galvanostatic charge (potential vs. time) profile at 0.05 mA/cm^2 for 3 hours, 5 hours, and 10 hours in the (a) aqueous and (b) hybrid electrolyte.

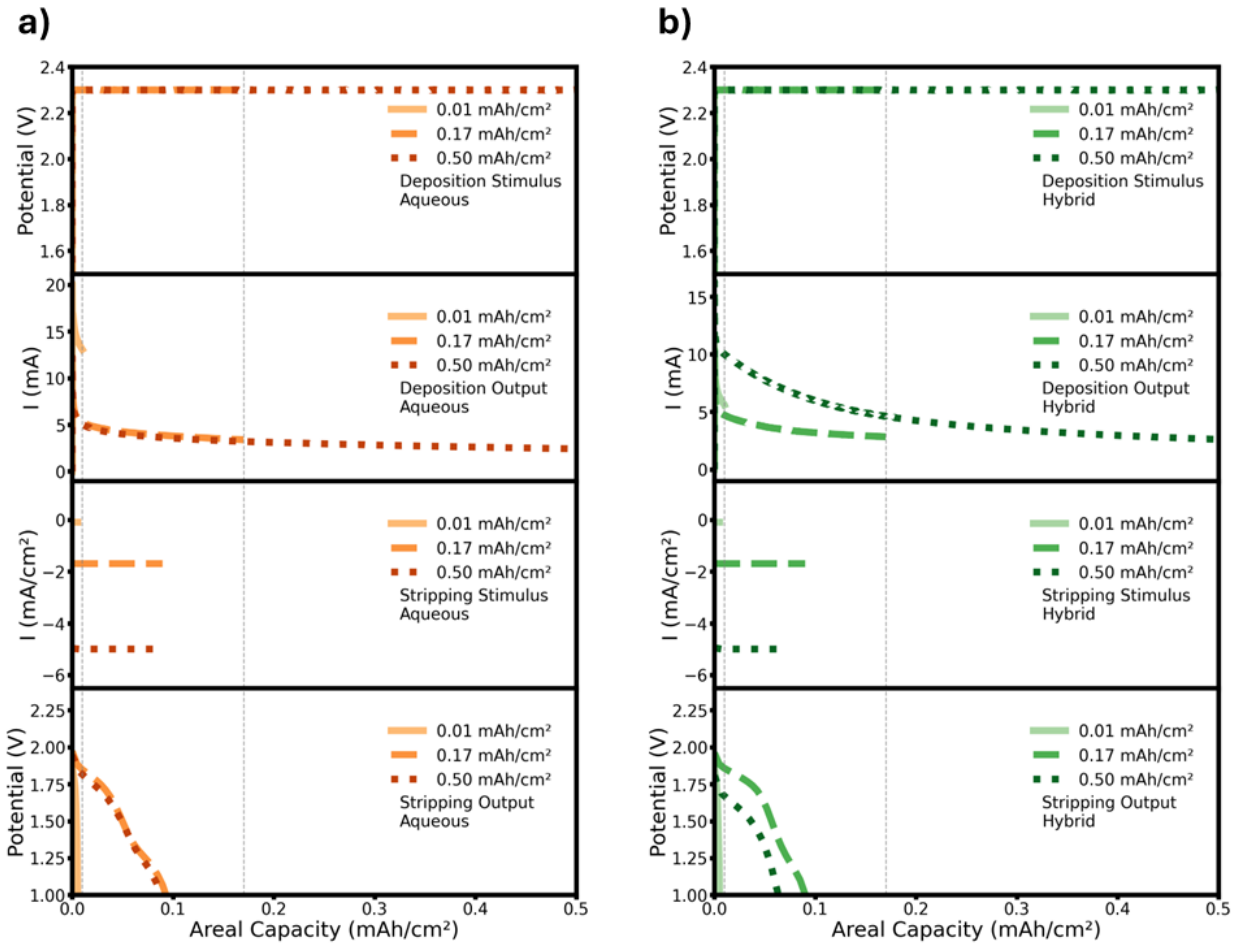

Figure S6. Chronoamperometric charge and galvanostatic discharge of initially anode and cathode-free Zn | MnO_2 batteries in (a) aqueous and (b) hybrid electrolytes. Each panel shows, from top to bottom, the applied potential during charge (V), the resulting current during charge(mA), the applied current density (mA/cm^2) during discharge, and the resulting potential during discharge (V) as a function of the areal capacity (mAh/cm^2). Dashed vertical lines indicate the target charging capacities of 0.01, 0.17, and 0.5 mAh/cm^2.

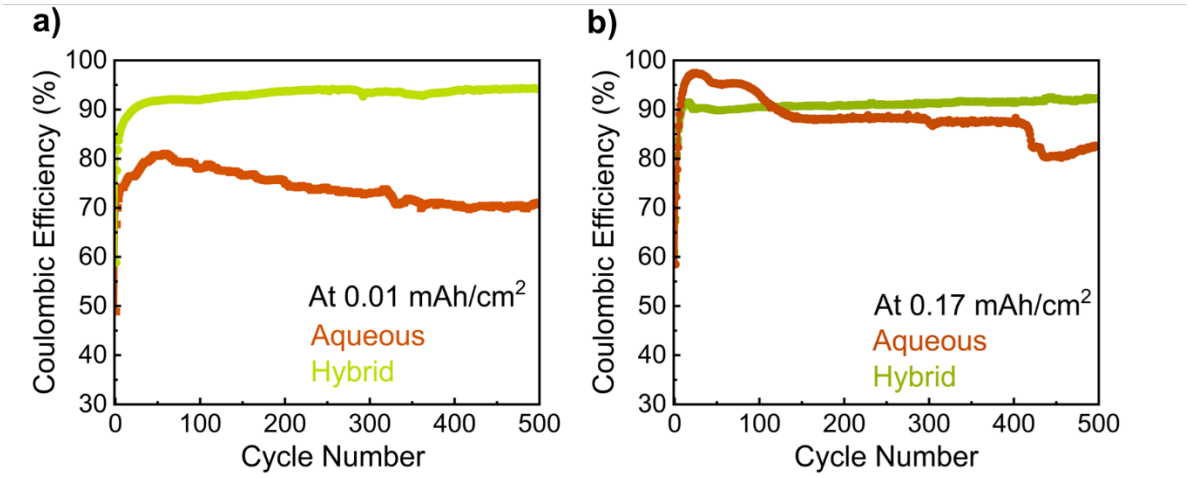

Figure S7. Long-term cycling of Zn/MnO_2 cells under a fast charging protocol (chronoamperometry at 2.3 V) at (a) charging capacity of 0.01 mAh/cm^2 and (b) charging capacity of 0.17 mAh/cm^2 in aqueous (orange) and hybrid (green) electrolytes. Coulombic efficiency (%) is plotted versus cycle number for 500 cycles.

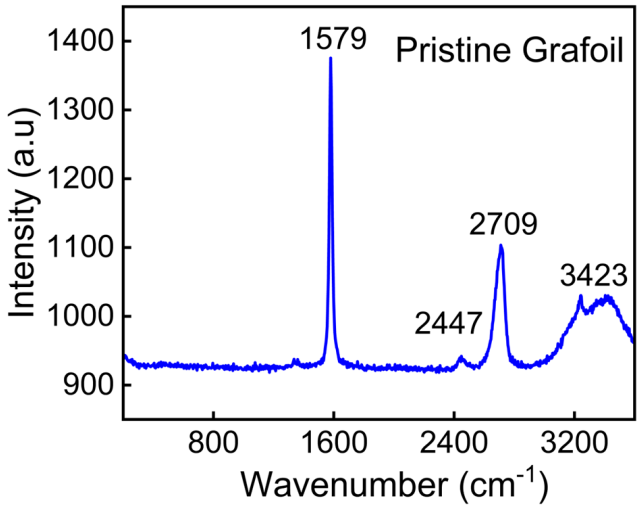

Figure S8. Ex situ Raman spectroscopy of pristine graphite foil performed with the water immersion lens, showing graphite peaks at 1579 cm^{-1} and 2709 cm^{-1} and a broad water peak at 3423 cm^{-1}.

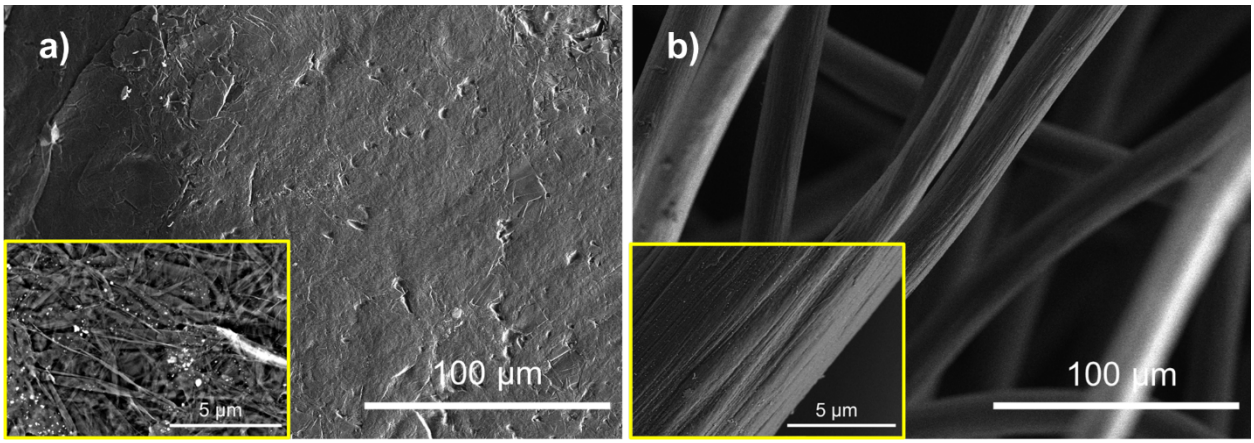

Figure S9. SEM images of (a) pristine graphite foil and (b) graphite felt.

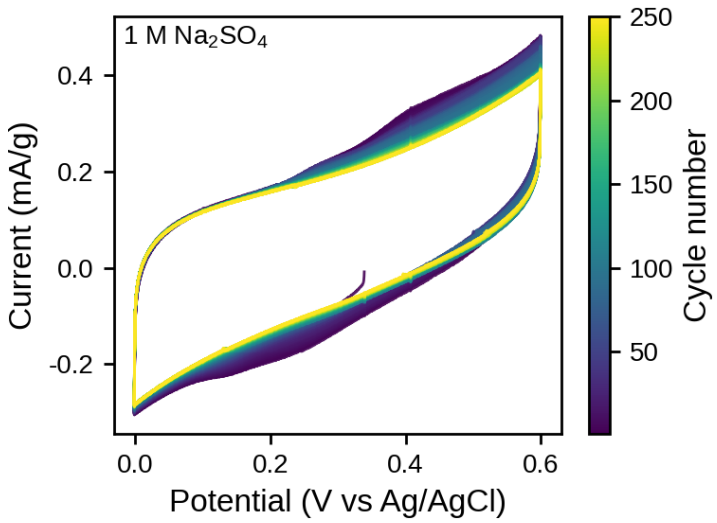

Figure S10. Cyclic voltammetry of porous graphite felt in a 1 M Na_2SO_4 aqueous electrolyte at 20 mV/s. Activated carbon served as the counter electrode and the reference electrode was Ag/AgCl in saturated KCl.

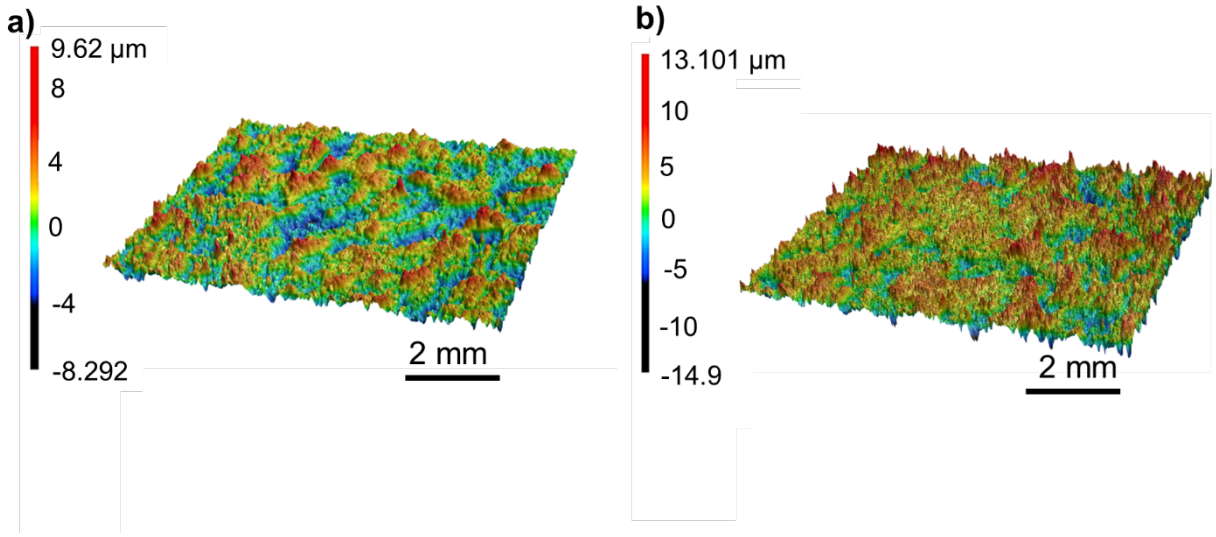

Figure S11. Laser optical microscopy of electrodeposited MnO_2 films at 0.17 mAh/cm^2 showing surface morphology and topography differences between (a) chronoamperometric deposition at 2.3 V and (b) galvanostatic deposition at 0.05 mA/cm^2. The 3D surface profiles reveal distinct roughness patterns and height variations (scale bar in µm) that reflect the influence of deposition protocol on surface roughness of electrodeposited MnO_2.

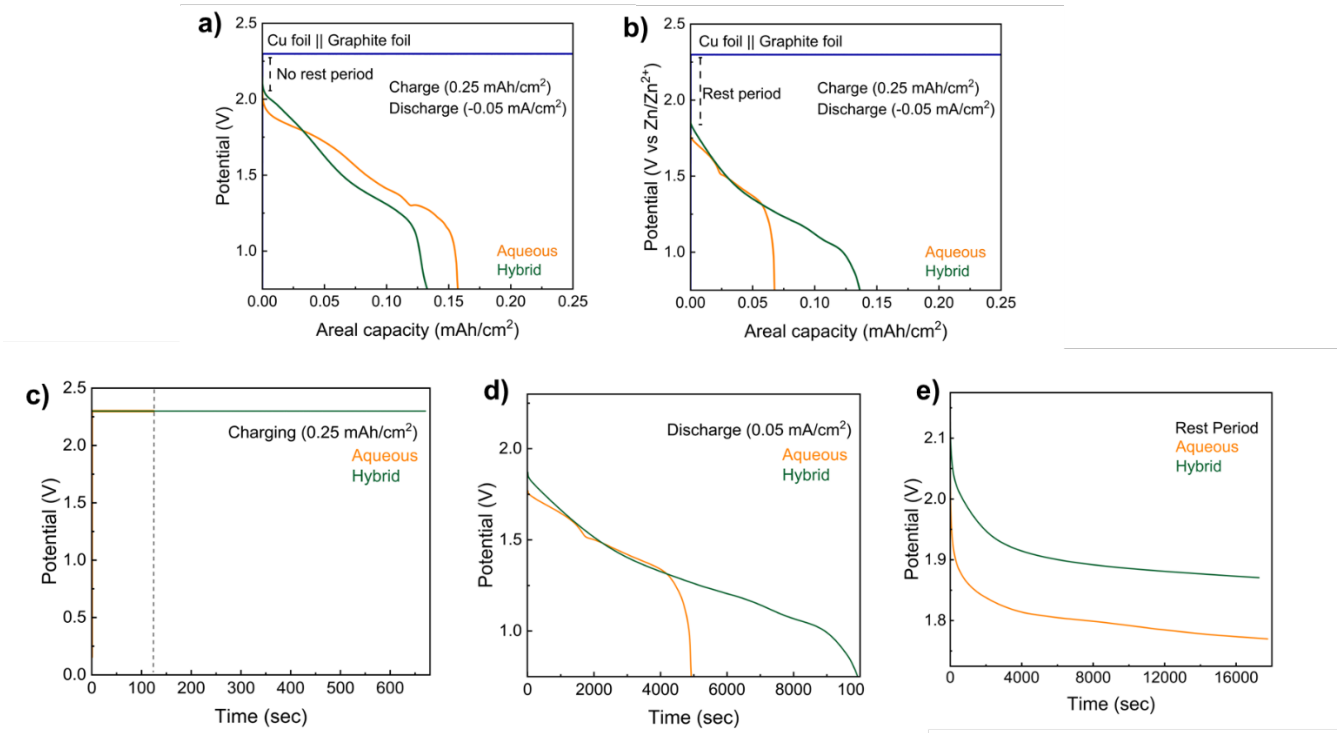

Figure S12. Chronoamperometric deposition at 2.3 V on graphite foil || Cu foil to a specific capacity at 0.25 mAh/cm^2 followed by (a) discharge at 0.05 mA/cm^2 (b) rest period ~4.8 hours and discharge at 0.05 mA/cm^2 to a cutoff voltage 0.75 V. Potential vs time profile of the (c) chronoamperometric charging at 2.3 V (d) 4.8 hours rest period and (e) discharge at 0.05 mA/cm^2 in aqueous and hybrid electrolyte.

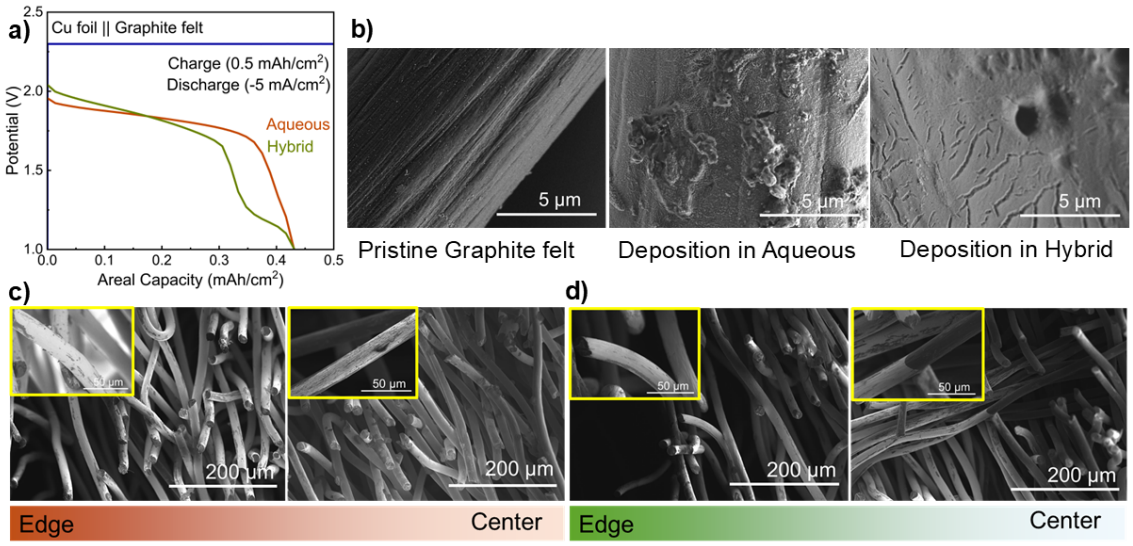

Figure S13. Porous graphite felt substrates deliver enhanced discharge utilization and distinct MnO_2 morphologies. (a) Galvanostatic discharge profiles after chronoamperometric deposition on graphite felt at 0.5 mAh/cm^2 in aqueous and hybrid electrolytes in Swagelok battery configuration (b) Plan-view SEM images of deposited MnO_2 at 0.5 mAh/cm^2 on graphite felt fibers in aqueous and hybrid electrolytes, revealing distinct morphological differences. Cross-sectional SEM images showing MnO_2 penetration depth and conformal coating from electrode edge to center in (c) aqueous and (d) hybrid electrolytes.

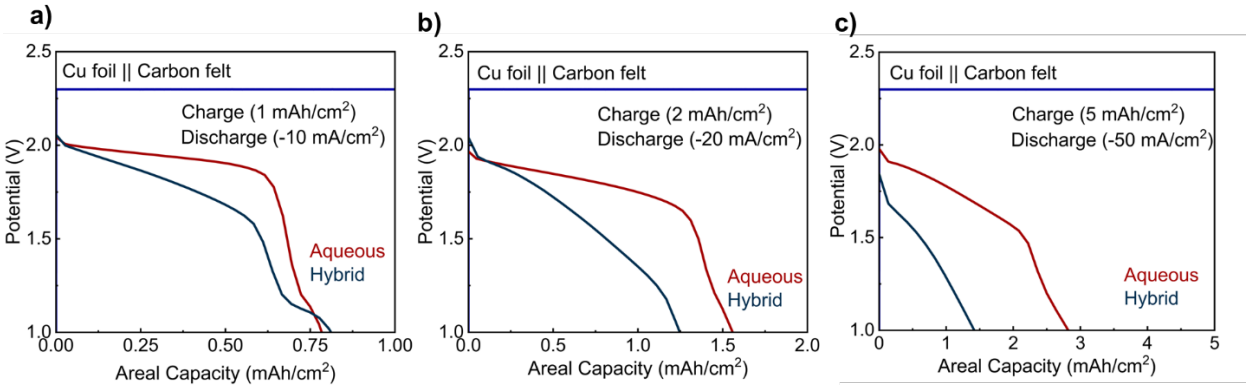

Figure S14. Galvanostatic discharge profiles after chronoamperometric deposition on Cu foil || graphite felt at (a) 1 mAh/cm^2, (b) 2 mAh/cm^2, and (c) 5 mAh/cm^2 in aqueous and hybrid electrolytes (Swagelok cell).

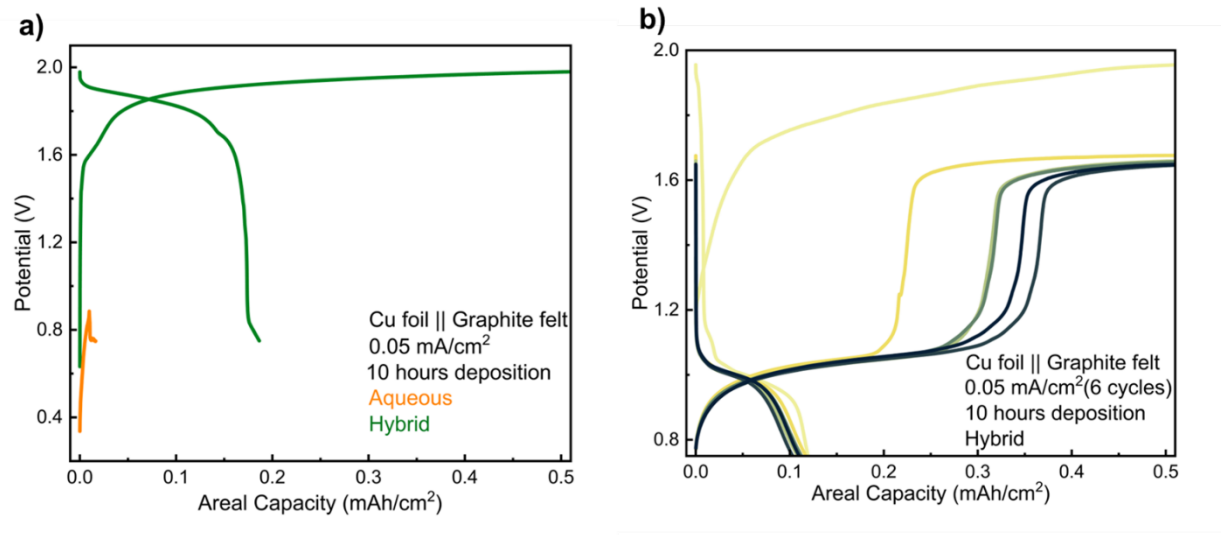

Figure S15. (a) Galvanostatic deposition/stripping of MnO_2 on porous substrate in the two-electrode Swagelok cell in aqueous and hybrid electrolyte. (b) Galvanostatic cycling (6 cycles) of Zn-MnO_2 in hybrid electrolytes in Swagelok cell configuration (Cu foil || Graphite felt).

2. Calculation of the Electrochemical Surface Area (ECSA) of Graphite Felt

The electrochemical surface area (A) of the porous graphite felt was estimated from the double layer capacitance (C_{dl}) of the graphite felt obtained in 1 M Na_2SO_4 at 20 mV/s. For 250th cycle, C_{dl} was calculated by taking the integral of the anodic current (I) between two voltages (in this example calculation V_1 = 0.25 V, V_2 = 0.45 V) and dividing by the scan rate (v) and voltage window (V_2-V_1):

$$C_{dl} = \frac{\int_{V_1}^{V_2} I dV}{v(V_2-V_1)} \quad \text{(S1)}$$

$$C_{dl} = \frac{1.868\times10^{-2}\ mC}{0.004\ V} \quad \text{(S2)}$$

$$C_{dl} = 4.67\ mF \quad \text{(S3)}$$

$$C_{dl} = 4.67\times10^{-3}\ F \quad \text{(S4)}$$

The porous carbon electrochemical surface area was then determined by assuming a surface-area normalized capacitance for carbon of 40 μF/cm^2.[1]

$$A = \frac{C_{dl}}{C_s} = 116.77 cm^2 \quad \text{(S5)}$$

The mass-normalized electrochemical surface area (A_M) was then obtained by dividing the electrochemical surface area A by the mass of the carbon scaffold (M):

$$A_M = \frac{A}{M} = \frac{1.1677\times10^{-2} m^2}{0.625\ g} = 0.0186\ m^2/g \quad \text{(S6)}$$

3. Supplementary Tables

Table S1. Thickness of electrodeposited MnO_2 following galvanostatic charge at 0.05 mA/cm^2 for 10 hours in aqueous and hybrid electrolytes, obtained from cross-sectional SEM.

Location	Deposition Thickness (μm) (Aqueous)	Deposition Thickness (μm) (Hybrid)
1	2.158	2.228
2	2.447	2.055
3	2.535	2.019
4	2.254	2.224

Table S2. Thickness of electrodeposited MnO_2 following chronoamperometric charging at 2.3 V for a total charge of 0.50 mAh/cm^2 in aqueous and hybrid electrolytes, obtained from cross-sectional SEM.

Location	Deposition Thickness (μm) (Aqueous)	Deposition Thickness (μm) (Hybrid)
1	2.597	3.985
2	2.482	4.252
3	2.623	4.458
4	2.623	5.512

Table S3. Video speed factors for operando electrochemical optical microscopy (normalized to experiment duration).

Plot	Zinc		MnO_2	
	Charge	Discharge	Charge	Discharge
CA+GCD BL	26.99x	23.25x	9.29x	24.47x
CA+GCD SL	52.48x	15.76x	43.03x	19.84x
Fast GCD BL	900x	900x	900x	900x
Fast GCD SL	900x	900x	900x	900x

Table S4. Surface roughness parameters of electrodeposited MnO_2 at 0.17 mAh/cm^2 (Figure S11) by chronoamperometric deposition at 2.3 V or galvanostatic deposition at 0.05 mA/cm^2. R_a is the arithmetical mean roughness and R_q is the root mean square roughness.

Surface Roughness	Chronoamperometric Deposition	Galvanostatic Deposition
R_a (μm)	2.656 ± 0.196	1.471 ± 0.139
R_q (μm)	3.516 ± 0.255	1.965 ± 0.169

4. Supplementary Reference

[1] B. E. Conway, in *Electrochemical Supercapacitors: Scientific Fundamentals and Technological Applications*, ed. B. E. Conway, Springer US, Boston, MA, 1999, pp. 221–257.